J. Eng. Technol. Sci., Vol. 53, No. 1, 2021, 210102

Site Test Performance and Numerical Study of Vertical Axis Hydrokinetic Turbine Straight Blade Cascaded (VAHT–SBC)

Ridho Hantoro*, Sarwono, Fernando Parsaulian Panjaitan, Erna Septyaningrum & Nuril Hidayati

Engineering Physics Department, Institut Teknologi Sepuluh Nopember Surabaya, Campus ITS Sukolilo, 60111, East Java, Indonesia
*E-mail: hantoro@ep.its.ac.id

Highlights:

- This study designed a hydrokinetic energy conversion system (HECS), which connects a permanent magnetic synchronous generator with a vertical axis turbine through a pulley and belt transmission system.
- The developed model of the Vertical Axis Hydrokinetic Turbine – Straight Blade Cascaded (VAHT-SBC) can potentially produce a maximum power potential of 174.058 W on site with a current velocity of 0.92 m/s, however, in this condition the turbine efficiency is the lowest (22.25%).
- A pulley ratio of 1:3 had the highest performance in this integration system, due to its ability to generate a load of 50 W on site with a current velocity of 0.82 and 0.92 m/s.

Abstract. The Vertical Axis Hydrokinetic Turbine – Straight Blade Cascaded (VAHT-SBC) is a type of energy generation technology developed to meet the increasing demand for renewable energy. Previous studies have been carried out to enhance the efficiency of the turbine through several aspects. To deploy a turbine on site, a study on its power generation and conversion is needed. In this research, the VAHT–SBC was integrated with a permanent magnet synchronous generator (PMSG) by a pulley and belt transmission system. This study was conducted by experimental and numerical analysis. The CFD simulation result showed that the highest torque of the turbine was found at 0° and 360°, with an average value of 23.923 Nm and with current velocity at 0.92 m/s. The experimental data showed that the voltage and frequency were proportional to the generator rotational speed and inversely correlated with the load given to the integration system. In the inverter, the voltage and frequency values were stable at 230 V and 56 Hz respectively. The VAHT-SBC prototype was able to produce a maximum power of 50 W on site, with a current velocity of 0.82 and 0.92 m/s.

Keywords: *hydrokinetic energy conversion; load; PMG; rotational speed; VAHT-SBC; voltage.*

Received January 30th, 2020, 1st Revision June 19th, 2020, 2nd Revision Juy 12th, 2020, Accepted for publication September 17th, 2020.

DOI: 10.5614/j.eng.technol.sci.2021.53.1.2

1 Introduction

An alternative to reducing our carbon footprint is by massive adoption of renewable energy to fulfill the market's demand. A relatively cheap source of renewable energy is hydropower. The utilization of kinetic energy from water is called hydrokinetic energy, which can be installed on various types of energy resources, such as rivers, ocean currents, and waves [1]. The technology to extract hydrokinetic energy is the turbine [2], which has the same electricity generation mechanism as a wind turbine [3].

The hydrokinetic turbine is a suitable option for energy extraction at low speed, it is omnidirectional (independent to current direction), easy to maintain, and does not require a yaw mechanism [4-7]. Based on their axis, hydrokinetic turbines are divided into two types, namely horizontal axis turbines (HAT) and vertical axis turbines (VAT) [8]. The lift force-based turbine has superiority due to the streamlined blades of its rotor, which reduces the backward drag force and enhances the lift force generated [9]. Studies on the shape of the blades have been conducted to further improve its performance, proposing straight blades, helical blades, troposkein curved blades, crooked helical blades, including Gorlov turbines with V-blades [10-14]. Researchers have also studied hybrid hydrokinetic turbines, such as a hybrid between the Darrieus and the Savonius rotor to overcome its low efficiency and self-starting issues [15-17].

In addition to that, experimental and numerical studies have been carried out to investigate the blade configuration design [18-20]. The results showed that a 9-blade configuration consisting of a passive-pitch blade as the outer blade and a fixed-blade for the other blades had the highest coefficient of power, i.e. 0.42, which is 93% of its theoretical value. Hence, the present study continued to explore the systems needed to support this specifically designed turbine installation, i.e. the energy conversion and transmission systems. To meet the energy required by the grid, a hydrokinetic turbine needs to convert the mechanical energy produced by the rotation of the turbine into electrical energy using a generator and a power converter. Characteristics that need to be satisfied according to the gird qualifications are frequency, voltage, active and reactive power control, and harmonics [21]. There are several types of generators that can be integrated with a hydrokinetic turbine, one of which is the permanent magnet synchronous generator (PMSG) [22-23]. The PMSG is frequently used on wind turbines due to its high performance at variable speed, including high efficiency and high control capabilities of the power generation system [24].

The second system required to operate a hydrokinetic turbine is the transmission mechanism to integrate the turbine with the generator. Its function is to transmit the torque and rotating energy of the turbine to the generator. The transmission

mechanism that was used in this study was a pulley and belt mechanism. When compared to a gearing system, a previous study has proven that on average the pulley and belt mechanism is more feasible in terms of cost and power production [25].

The energy conversion system from a hydrokinetic turbine has unique characteristics, such as its fluctuating torque, which affects the performance of the generator, and its high torque with a low rpm value. As this research reached the implementation stage, a specified energy conversion system was designed to support the performance of the VAHT SBC with its special characteristics. This research studied the integration between the innovated vertical axis hydrokinetic turbine with a PMSG energy conversion and pulley and belt transmission mechanism. The energy conversion and transmission mechanisms were assessed experimentally to find out the characteristics of the generator, i.e. rotational speed, voltage, and frequency in accordance with the variation of the load and the pulley ratio. Another expected primary result was the potential power that could be produced by the turbine. A minor numerical analysis study was carried out to extract the turbine performance parameters that were unable to be drawn from the experiment, i.e. the distribution profile of velocity and pressure. Although this work used a VAHT-SBC, it is expected that it can also contribute to the design of mechanical to electrical conversion systems for various types of hydrokinetic turbines and other types of renewable energy technology with similar characteristics.

2 Design and Construction for Hydrokinetic Energy

2.1 Design of Hydrokinetic

Prior this study, deep research has been conducted to enhance vertical turbine performance by innovating the cascade blade by combining the fixed and the passive pitch, as depicted on Figure 1. This model will be referred to as straight blade cascaded (SBC). This modification succeeded to tackle the low efficiency and self-starting issues of vertical axis turbines [18-20]. This combination allows the turbine to have greater force and torque as well as a larger area so that the pressure will be higher [26]. Besides, the SBC is useful to increase the turbine's power extraction without enlarging its dimensions [11].

VAHT-SBC has nine blades with three blades on each arm. The outer blade on each arm has a passive-pitch mechanism, which enables the blades to adjust their pitch angle in the range of $-20° \leq \beta \leq 20°$ [19-20]. The aspect ratio of the turbine is 1:8 with chord and span length at 10 cm and 80 cm, respectively, using NACA 0018 as hydrofoil profile. The hydrofoil is fabricated using an iron plate layered

by resin fiber composite, which is essential to achieve a similar blade shape as NACA 0018.

Figure 1 Design of the VAHT-SBC.

2.2 Design of Hydrokinetic Power Generation System Integration

The hydrokinetic energy conversion system (HECS) as depicted in Figure 2 was adapted from wind energy system conversion (WESC). The generator and the electrical system in the HESC play a essential role in converting the mechanical energy of the turbine to electrical form.

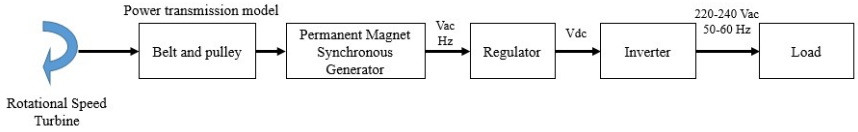

Figure 2 Block diagram of the power conversion system.

A transmission element is used to connect the rotating system. In this research, the type of transmission system used was a pulley and belt transmission system, as shown in Figure 3. This type of transmission connects the turbine shaft with a shaft moved by a belt. The pulley used by the generator was 5.08 cm in diameter, while the turbine pulley varied by 15.24 cm, 20.32 cm, and 25.4 cm. Thus, the pulley ratios were 1:3, 1:4, and 1:5 respectively. The pulley applied on the turbine was a driving pulley, while the pulley applied on the generator was a driven pulley. The generator is one of the most important components in an HESC because it determines the power generated. This research utilized a permanent magnet synchronous generator (PMSG) for its high performance with a capacity of 600 W and 650 RPM as its highest rotational speed. Its rated torque is 0.52 Nm, while the rated and excitation voltage are 12/24/48 V and 0-220 Vdc,

respectively. This three-phase generator, which generates AC voltage, was connected to a rectifier.

Figure 3 Belt and pulley transmission system with a ratio of 1:5.

The components of the converter system consisted of a three-phase rectifier, a step down voltage regulator, and an inverter. The output of the three-phase rectifier used was DC voltage. The step-down voltage was used to lower the voltage input from the rectifier to 14.5 Vdc as the standard of the inverter. In this research, the capacity of the voltage regulator was set to 200 W with 60 Vdc as the highest input. This selection of the regulator was based on the turbine capacity to extract hydrokinetic energy. The last component to convert the current, voltage, and frequency to meet the given load is an inverter. The inverter output was AC current with sine wave modified voltage and a capacity of up to 500 W. In an applied hydrokinetic system, the output of the inverter is transmitted to the grid. However, because the main objective of this research was to assess the performance of the integrated system, the grid was replaced by a dummy load instead.

3 Numerical Study and Site Test Performance Setup

3.1 Simulation Setup

To gain the data and profile of the parameters that could not be obtained experimentally, a computational fluid dynamic (CFD) simulation based on the Reynold Average Navier-Stokes (RANS) solver was conducted. The RANS solver is a coupled flow solver that simultaneously solves the momentum and continuity equations [27]. The simulated geometry consisted of a rotational and a stationary domain, representing the rotating turbine and the channel.

The dimension of the stationary domain was 3D x 10D m, where D is the diameter of the turbine. The turbine was located 3.5D from the inlet [4,19,28] with its dimensions listed in Table 1. The boundaries of the stationary domain were defined as inlet, outlet, opening for the upper site, and wall for the channel wall

and base, as presented in Table 2. After the design process of the geometry, meshing was conducted to generate the control volumes where the calculation of equations occurred, as shown in Figure 4. However, a turbulence model study needed to be done first, to provide the proper model for this simulation. Thus, a test with 15 variations in total was conducted, as presented in Table 3. The mesh size settings were coarse, medium, and fine, while the turbulence models used for the setting were laminar, K epsilon, SST, BSL Reynold stress, and SSG Reynold stress.

Table 1 Dimensions of the VAHT-SBC.

Parameter	VAHT-SBC
Cord length	0.1 m
Span	0.8 m
Diameter	0.8 m
H/D	1
Aspect ratio	8
Hydrofoil	NACA 0018

Table 2 Boundary condition setup.

Inlet	Current velocity as the experiment sites (0.74, 0.82, 0.92 m/s)
Outlet	Opening
Wall	Opening
Turbine (blades and shaft)	Rotating Wall – no slip
Lower surface	Wall – no slip
Upper surface	Wall – no slip

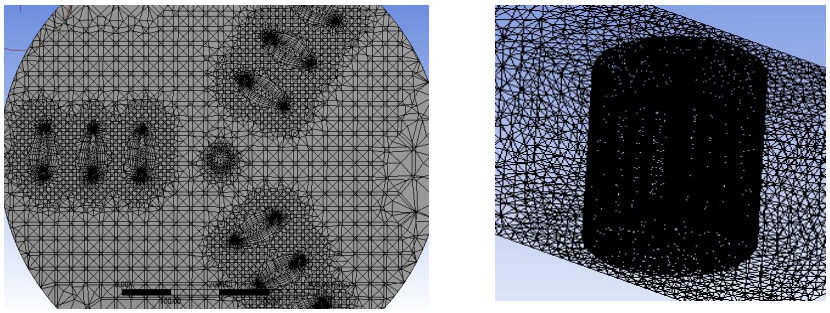

(a) (b)

Figure 4 Grid generation in (a) blade (top view); (b) all domains.

The test result showed that the configuration that gave the smallest error was the meshing with fine sizing and the SST turbulence model, with an error of 2.59%. The error represents the difference in torque between the CFD simulation and the experimental data. The result of the turbulence model testing was aligned with

previous CFD studies [19,28-31], which state that the most representative turbulence model for fluid-solid interaction simulation is SST. This model optimizes the strength of the k-ω and k-ε turbulence model and eliminates its weakness.

Table 3 Turbulence model meshing test.

Setting	Number of element	Average skewness	Turbulence model	Deviation (%)
Coarse	3141062	0.57	Laminar	33.73
			K epsilon	25.44
			SST	15.83
			BSL Reynold *Stress*	21.80
			SSG Reynold *Stress*	18.15
Medium	3512214	0.48	Laminar	16.15
			K epsilon	13.10
			SST	3.18
			BSL Reynold *Stress*	12.52
			SSG Reynold *Stress*	14.51
Fine	4862183	**0.30**	Laminar	10.53
			K epsilon	7.22
			SST	**2.59**
			BSL Reynold *Stress*	5.23
			SSG Reynold *Stress*	13.18

The next step was a gird dependency test to determine the optimal grid, as tabulated in Table 4. Based on this table, the present study used a mesh setting with 4,862,183 elements. There were various grid sizes for each domain. The grid size of the rotating domain and the turbine were smaller because the detailed calculation occurred in these domains. The turbulence model and grid dependence test were run for a current velocity of 0.74 m/s of site A.

Table 4 Grid dependency test.

Number of Elements	Orthogonality	Torque
3,755,643	0.852	19.86
4,476,906	0.861	20.13
4,862,183	0.905	23.37
5,532,165	0.920	23.39

This work also analyzed the y+ of various mesh settings. Figures 4(a) and 4(b) represent the y+ graph of mesh settings with 3,755,643 and 4,862,183 elements. The value of y+ in the graph shows that the position of the first node from a larger grid size resulted in more fluctuation. This affected the increment of shear stress, which resulted in a greater value of C_D compared to the y+ of the smaller grid size.

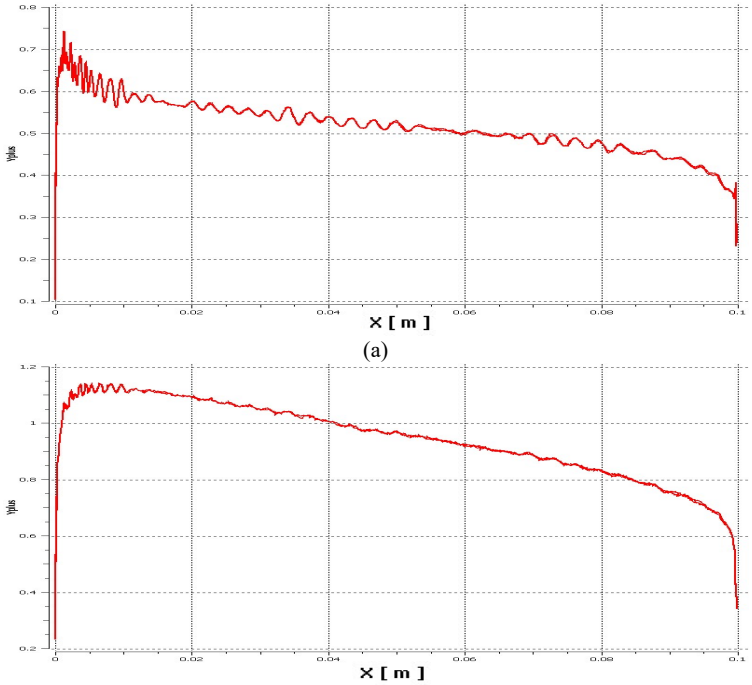

Figure 5 Y+ of mesh with (a) 3,755,643 (b) 4,862,183 elements.

The CFD simulation was validated with the torque of the experimental data, with an average error rate of the computational fluid dynamic of 5.49%, as presented in Table 5. A different result was obtained because the numerical model was considered ideal, whereas the possibility of encountering losses along the experimental process was high. Nevertheless, the error was below 10%, which confirms the validity of the simulation.

3.2 Site Test Setup

A site test of hydrokinetic power generation performance was done experimentally in an open channel located at PDAM Umbulan Pasuruan. This site is suitable for hydropower turbine implementation since it has untapped hydrokinetic potential. It has 0.97 m width and 1.55 m depth with a current velocity of 0.74-0.92 m/s. The detailed results of the site test are presented in Table 5. For the site test, three sites with different flow velocities were chosen as the test locations. The current velocity of the open channel was measured by using a Dentan CM-IBX series current meter, which was placed 0.5 m upstream from the turbine frame. There were 5 collected data for each measurement point.

Table 5 Data of torque from experiment and CFD simulation.

Location	Current velocity (m/s)	Rotational speed (rpm)	Experimental torque (Nm)	Simulation torque (Nm)	Error (%)
Site A	0.74	61.736	23.923	23.37	2.59
Site B	0.82	63.156	25.154	23.83	6.3
Site C	0.92	63.772	26.077	24.1	7.58

A JTN 4603BN torque wrench was used to measure the torque of the turbine. The torque wrench was locked to the tip of the turbine to measure the torque for every 30° shift in azimuth angle. The presented torque data in Table 5 are the average values of a total of 13 azimuth angles. For each azimuth angle, the data were retrieved 5 times.

The rotation speed of the turbine and generator were measured by a WIPRO DT 2235A tachometer with a unit of radian per second. The three experiments were measured using a tachometer, including the rotation of the turbine in the channel, the rotation of the generator coupled to a motor and when its rotation declined due to the load, and the integrated turbine and generator before and after loading. For every current velocity, the rotational speed data were retrieved 5 times. For the electrical aspects, the data needed were the value of the voltage and the frequency at the input and output of each component measured by a multimeter. Because the generator used was a three-phase generator it was necessary to measure the line to line voltage to find out the balance between lines R, S, and T. The electrical data were retrieved three times for each presented data.

4 Result and Discussion

4.1 Turbine Performance

The turbine performance needed to be assessed prior to the installation of the mechanical transmission and electrical system. The fluctuating torque and low RPM characteristic was considered for the mechanical to electrical conversion system. The correlation among current velocity, torque, and rotational speed is presented in Table 5. Among the three data retrieved from the experiment presented in Table 6, the data of current velocity had the lowest average percentage of uncertainty at 2.15%. The average uncertainty of rotational speed and the torque data from sites A, B, and C were 4.461% and 4.697% respectively. The highest current velocity was found at site C with the highest torque and rotational speed of the turbine. The turbine produced 23.923 Nm, 25.154 Nm, and 26.077 Nm at sites A, B and C respectively.

Table 6 Uncertainty of experimental data.

Site	Current velocity	Rotational speed	Torque
Site A	2.449%	4.445%	4.941%
Site B	2.000%	4.285%	4.352%
Site C	2.000%	4.652%	4.799%
Average	2.150%	4.461%	4.697%

The torque data were used to determine the power generated by the turbine. Thus, it was used to measure the performance coefficient (Cp) as the ratio between the power generated by the turbine and the potential power of water. Moreover, the power data were used to determine the specifications of the generator and the other electrical systems. The power generated was highest at site C (174.058 W) with an inlet current velocity of 0.92 m/s, which proves that the increment of power produced by the turbine is proportional to rpm and torque. In contrast, the turbine power is inversely proportional to the resulting power coefficient value. This is because the potential power of water is a function of current velocity with the power of three. The efficiency of the turbine at sites A, B, and C in sequence was 37.9%, 30%, and 22.25%. These data could be utilized to determine the power conversion system that was installed into the integration system.

In addition to the torque from the experiment data, the numerical study yielded the detailed torque fluctuation for each azimuth angle. Based on the data presented in Figure 6, the highest torque was observed for azimuth 0° and 360°, where the turbine arm is at a right angle from the water inlet, causing a large torque value because of the high amount of force received.

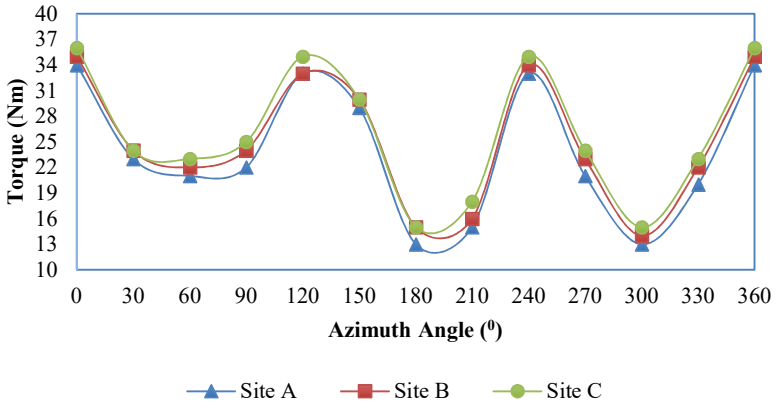

Figure 6 Torque fluctuation.

Besides torque, the result of the numerical analysis showed the contours of the velocity streamline and pressure as presented in Figure 7. There was a pressure difference in the area around the foil with the highest value on Foil I, which then gradually decreased near the other foils. The higher the pressure on the foil side, the higher the force on the foil, which results in a higher shaft rotational speed and torque. The streamline profile shown in Figure 7 shows the flow direction of the current velocity in the turbine. The current velocity was highest at the rotation edge of the turbine (3.45 m/s) due to the rotation effect of the rotating turbine.

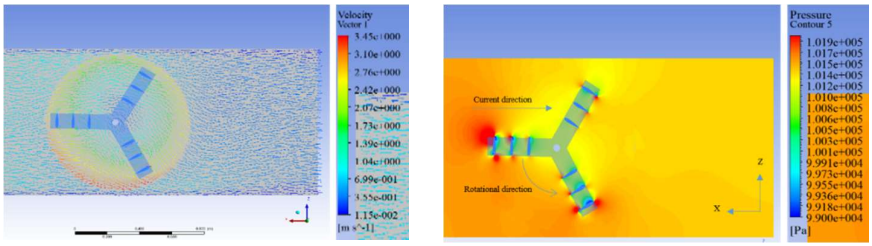

(a) (b)

Figure 7 Contour of (a) streamline profile and velocity vector, (b) pressure.

4.2 Hydrokinetic Energy Conversion System Performance

Since the highest power was generated at site C, the presented data on the hydrokinetic energy conversion system were drawn from site C only. A pulley and belt system was selected as the mechanical and transmission system considering its fabrication and installation are easily done. This system ensures that the resulting rpm and torque are in the range of the generator's rpm and torque. This is important, as the hydrokinetic turbine has a very low rpm compared to the generator requirement. Figure 8 shows the average result of the turbine and generator rpm that was connected to the turbine at the various pulley ratios. The smaller the pulley ratio, the lower the rpm resulted from the mechanical transmission, which also influences the torque output of the mechanical transmission system.

For each pulley ratio, the given load was different due to the effect of the torque generated by the motor, which was inversely proportional to the pulley diameter and rpm, as presented in Figure 8. Meanwhile, the value of the output voltage of the generator, the three-phase rectifier, the voltage regulator, and the inverter were different for each pulley ratio. Characteristically, the voltage of the generator and inverter are alternating current, while the voltage of the rectifier and regulator are direct current.

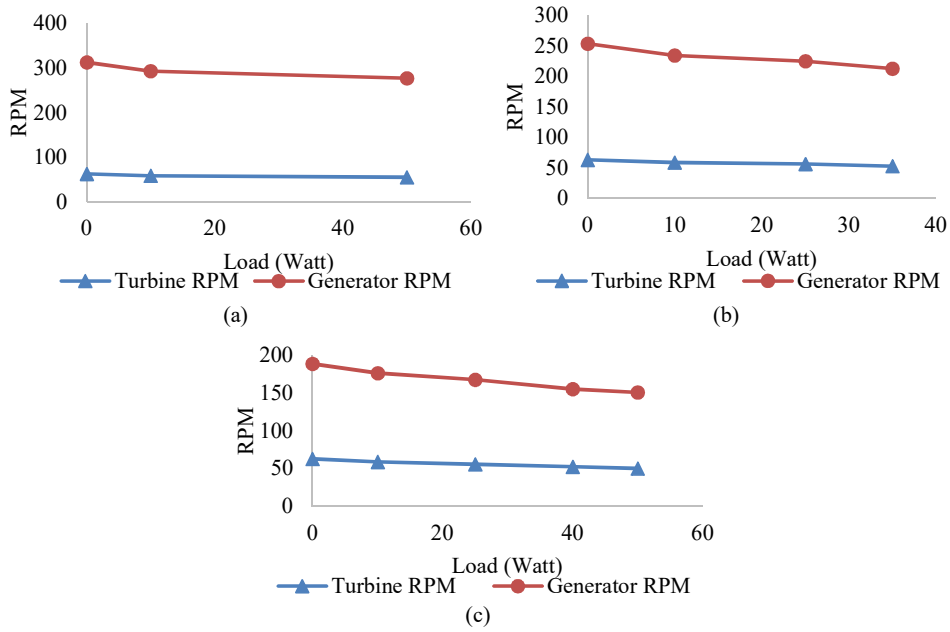

Figure 8 Rpm for various loads: (a) at pulley ratio 1:5, (b) at pulley ratio 1:4, (c) at pulley ratio 1:3.

The value of voltage had a linear correlation with rpm, except for the output voltage of the regulator and the inverter, which were constant at 15.5 Vdc and tended to be stable at 232-233 Vac. As the rpm decreases, the output frequency of the generator will decrease as well, which leads to a decrease of the voltage since the voltage of the generator is a function of its rotation. However, this did not apply to the inverter, which had a stable frequency of 56 Hz.

In the loading cases, the increment of load also increased the work of the generator, which led to an increase of the electric current needed. The voltage of all elements decreased with the rise of the load, as presented in Figure 9. A small amount of decrement was found for the voltage regulator with 0.01-0.04 Vdc. This decline was caused by an increment of the electric current supplying the load. Besides, the increment of the load decreased the frequency of the generator but increased the frequency of the inverter. However, the inverter frequency fluctuation was insignificant.

For the HECS used in this work, the experimental data showed that the highest power potential that could be extracted by the VAHT-SBC was 50 W. This value was found in two points, namely site B (0.82 m/s) and site C (0.92 m/s) with a

pulley ratio of 1:3. These high power values followed the high turbine torque and high generator rpm. Meanwhile, the power that could be extracted from the power conversion system at site A was 40 W.

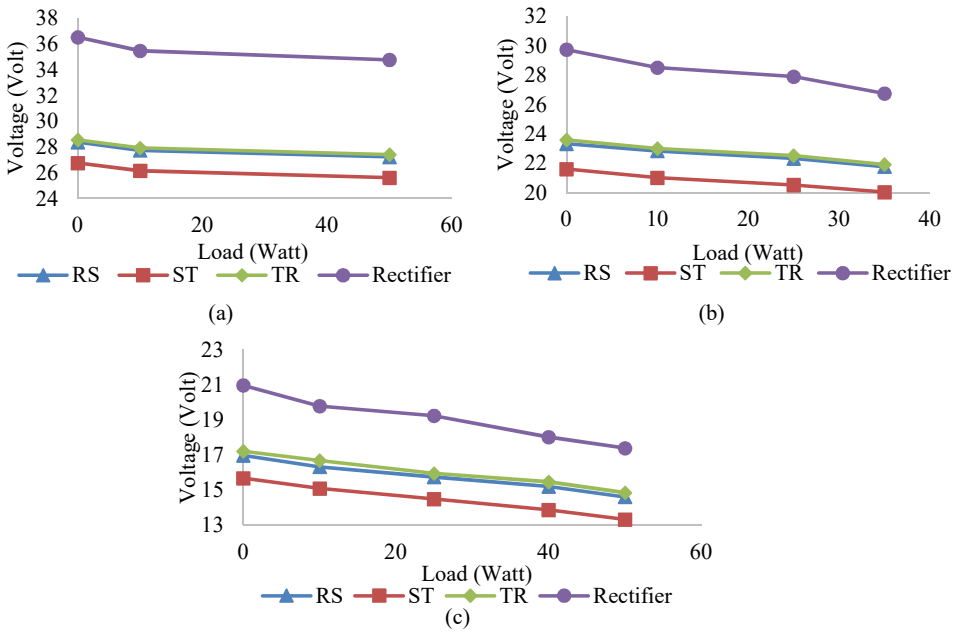

Figure 9 Voltage output of the generator and the rectifier for various loads: (a) at pulley ratio 1:5 (b) at pulley ratio 1:4, (c) at pulley ratio 1:3.

5 Conclusion

From the three sites assessed in this study, site C with a current velocity of 0.92 m/s stored a hydrokinetic power potential of 174.058 W, however, the turbine efficiency of 22.25% at that site was the lowest. The designed hydrokinetic energy conversion system connected the permanent magnetic synchronous generator with the turbine through a pulley and belt transmission system. Based on the experimental data, the voltage of the generator and rectifier output was proportional to the rpm value. The voltage at the output regulator and inverter accounted for 17.5 Vdc and 232-233 Vac, respectively. The frequency of each component was proportional to the rpm value, except for the inverter, which was constant at 56 Hz. The loading is inversely proportional to the voltage and frequency, but has a linear correlation with the frequency of the inverter. The highest power potential that could be extracted by the VAHT-SBC was 50 W, found at site B (0.82 m/s) and site C (0.92 m/s) with a pulley ratio of 1:3.

Acknowledgement

This research was supported by LPPM ITS. The authors would like to thank the Energy Engineering and Environmental Conditioning Laboratory of Engineering Physics, ITS for the facilities provided to complete this research.

References

[1] Lago, L., Ponta, F. & Chen, L., *Advances and Trends in Hydrokinetic Turbine Systems*, Energy for Sustainable Development, **14**(4), pp. 287-296, 2010.

[2] Guney, M.S. & Kaygusuz, K., *Hydrokinetic Energy Conversion System: A Technology Status Review*, Renewable and Sustainable Energy Reviews, **14**(9), pp. 2996-3004, 2010.

[3] Hu, Z. & Du, X., *Reliability Analysis for Hydrokinetic Turbine Blades*, Renewable Energy, **48**, pp. 251-262, 2012.

[4] Posa, A., Parker, C.M., Leftwich, M.C. & Balaras, E., *Wake Structure of a Single Vertical Axis Wind Turbine*, Int. J. Heat Fluid Flow, **61**, pp. 75- 84, 2016.

[5] Ross, I. & Altman, A*., Wind Tunnel Blockage Corrections: Review and Application to Savonius Vertical-axis Wind Turbines*, J. Wind Eng. Ind. Aerodyn., **99**(5), pp. 523-538, 2011.

[6] Tescione, G., Simao Ferreira, C.J. & van Bussel, G.J.W., *Analysis of a Free Vortex Wake Model for the Study of the Rotor and Near Wake Flow of a Vertical Axis Wind Turbine*, Renew. Energy, **87**, pp. 552-563, 2016.

[7] Beri, H. & Yao, Y., *Double Multiple Streamtube Model and Numerical Analysis of Vertical Axis Wind Turbine*, Energy Power Eng., **3**(3), pp. 262-270, 2011.

[8] Khan, M.J., Bhuyan, G., Ipbal, M.T. & Quaicoe, J.E., *Hydrokinetic Energy Conversion Systems and Assesment of Horizontal and Vertical Axis Turbine for River and Tidal Applications: A Technology Status Review*, Applied Energy, **86**(10), pp. 1823-1835, 2009.

[9] Saini, G. & Saini, R.P., *A Review on Technology, Configurations, and Performance of Crossflow Hydrokinetic Turbines*, International Journal of Energy Research. 2019. DOI: 10.1002/er.4625.

[10] Scheurich, F., Fletcher, T.M. & Brown, R.E., *The Influence of Blade Curvature and Helical Blade Twist on the Performance of a Vertical-axis Wind Turbine*, AIAA Aerospace Sciences Meeting Including the New Horizons Forum and Aerospace Exposition, Orlando, 2013.

[11] Kirke, B.K., *Tests on Ducted and Bare Helical and Straight Blade Darrieus Hydrokinetic Turbines*, Renewable Energy, **36**(11), pp. 3013-3022, 2011.

[12] Castelli, M.R. & Benini, E., *Effect of Blade Inclination Angle on a Darrieus Wind Turbine*, Journal Turbomach, **134**(3), pp. 1-10, 2011.
[13] Yang, B. & Lawn, C., *Fluid Dynamic Performance of a Vertical Axis Turbine for Tidal Currents*, Renewable Energy, **36**(12), pp. 3355-3366, 2011.
[14] Worstell, M.H., *Aerodynamic Performance of the 17 Meter Diameter Darrieus Wind Turbine*, Sandia National Laboratories, California, 1978.
[15] Saini, G. & Saini, R.P., *A Computational Investigation to Analyze the Effects of Different Rotor Parameters on Hybrid Hydrokinetic Turbine Performance*, Ocean Eng., **199**, 107019, 2020. DOI: 10.1016/j.oceaneng. 2020.107019.
[16] Saini, G. & Saini, R.P., *Comparative Investigations for Performance and Self-starting Characteristics of Hybrid and Single Darrieus Hydrokinetic Turbine*, in Energy Reports, **6**(Suppl. 2), pp.96-100, 2020. DOI: 10.1016/ j.egyr.2019.11.047.
[17] Saini, G. & Saini, R.P., *A Numerical Analysis to Study the Effect of Radius Ratio and Attachment Angle on Hybrid Hydrokinetic Turbine Performance*, Energy Sustain. Dev., **47**, pp.94-106, 2018. DOI: 10.1016/ j.esd.2018. 09.005.
[18] Hantoro, R., Prananda, J., Mahmashani, A.W., Septyaningrum, E. & Imanuddin, F., *Performance Investigation of an Innovative Vertical Axis Hydrokinetic Turbine – Straight Blade Cascaded (VAHT-SBC) for Low Current Speed*, in Journal of Physics: Conference Series, **1022**, 2018. DOI: 10.1088/1742-6596/1022/1/012022.
[19] Hantoro, R. & Septyaningrum, E., *Novel Design of a Vertical Axis Hydrokinetic Turbine-Straight-Blade Cascaded (VAHT-SBC): Experimental and Numerical Simulation*, J. Eng. Technol. Sci., **50**(1), pp.73-86, 2018. DOI: 10.5614/j.eng.technol.sci.2018.50.1.5.
[20] Hantoro, R., Utama, I.K.A.P., Arief, I.S., Ismail, A. & Manggala, S.W., *Innovation in Vertical Axis Hydrokinetic Turbine – Straight Blade Cascaded (VAHT-SBC) Design and Testing for Low Current Speed Power Generation*, in Journal of Physics: Conference Series, **1022**, 2018. DOI: 10.1088/1742-6596/1022/1/012023.
[21] Yogesh, M.N., *A Review on Power Electronics Application on Wind Turbines*, International Journal of Research in Engineering and Technology, **2**(11), pp. 360-376, 2013.
[22] Tiwari, A.R., Shewale, A.J., Gagangras, A.R. & Lokhande, N.M., *Comparison of Various Wind Turbine Generators*, Multidisciplinary journal of Research in Engineering and Technology, **1**(2), pp. 129-135, 2014.
[23] Muhida, R., Zaidi, A.F.A., Tamsir, A. & Irawan, R., *Design of A DC-AC Link Converter for 500W Residential Wind Generator*, Mechatronics, Electrical Power, and Vehicular Technology, **3**, pp. 95-102, 2012.

[24] Jose, J., *An Approach for The Dynamic Behavior of Hydrokinetic Turbines*, Energy Procedia, **75**, pp. 271-276, 2015.

[25] Hossain, A., Iqbal, A.K.M.P., Rahman, A., Arifin, M. & Maziar, M., *Design and Development of a 1/3 Scale Vertical Axis Wind Turbine for Electrical Power Generation*, in Journal of Urban and Environmental Engineering, **1**(2), pp. 53-60, 2007.

[26] Camara, M.S., Camara, M.B., Dakyo, B. & Gualous, H., *Permanent Magnet Synchronous Generators for Offshore Wind Energy System Linked to Grid-Modeling and Control Strategies*, in 16th International Power Electron. Motion Control Conference Expo PEMC 2014, 2014.

[27] Versteeg, H.K. & Malalsekera, W., *An Introduction to Computational Fluid Dynamics: The Finite Volume Method Approach*, Prentice Hall, 1996.

[28] Zhao, G., Yang, R.S., Liu, Y. & Zhao, P.F., *Hydrodynamic Performance of a Vertical-Axis Tidal-Current Turbine with Different Preset Angles of Attack*, J. Hydrodyn., **25**, pp.280-287, 2013. DOI: 10.1016/S1001-6058 (13)60364-9

[29] Arnold, M.M., *Simulation and Evaluation of the Hydroelastic Response of a Tidal Current Turbine*, Stuttgart: Institute of Aircraft Design University of Stuttgart, 2017.

[30] Rezaeiha, A., Kalkman, I. & Blocken, B., *CFD Simulation of A Vertical Axis Wind Turbine Operating at A Moderate Tip Speed Ratio: Guidelines for Minimum Domain Size and Azimuthal Increment*, Renew. Energy, **107**, pp.373-385, 2017. DOI: 10.1016/j.renene.2017.02.006.

[31] Septyaningrum, E., *Performance Analysis of Multi-Row Vertical Axis Hydrokinetic Turbine-Straight Blade Cascaded (VAHT-SBC) Turbines Array*, J. Mech. Eng. Sci., **13**(3), pp.5665-5688, 2019. DOI: 10.15282/ jmes.13.3.2019.28.0454.